





Prediction of Retear After Arthroscopic Rotator Cuff Repair Based on Intraoperative Arthroscopic Images Using Deep Learning

Sung-Hyun Cho,* MD, PhD , and Yang-Soo Kim,*[†] MD, PhD 

Investigation performed at Department of Orthopedic Surgery, Seoul St. Mary's Hospital, The Catholic University of Korea, Seoul, Republic of Korea

Background: It is challenging to predict retear after arthroscopic rotator cuff repair (ARCR). The usefulness of arthroscopic intraoperative images as predictors of the ARCR prognosis has not been analyzed.

Purpose: To evaluate the usefulness of arthroscopic images for the prediction of retear after ARCR using deep learning (DL) algorithms.

Study Design: Cohort study (Diagnosis); Level of evidence, 2.

Methods: In total, 1394 arthroscopic intraoperative images were retrospectively obtained from 580 patients. Repaired tendon integrity was evaluated using magnetic resonance imaging performed within 2 years after surgery. Images obtained immediately after ARCR were included. We used 3 DL architectures to predict retear based on arthroscopic images. Three pretrained DL algorithms (VGG16, DenseNet, and Xception) were used for transfer learning. Training and test sets were split into 8:2. Threefold stratified validation was used to fine-tune the hyperparameters using the training data set. The validation results of each fold were evaluated. The performance of each model in the test set was evaluated in terms of accuracy, area under the receiver operating characteristic curve (AUC), F1-score, sensitivity, and specificity.

Results: In total, 1138 and 256 arthroscopic images were obtained from 514 patients and 66 patients in the nonretear and retear groups, respectively. The mean validation accuracy of each model was 83% for VGG16, 89% for Xception, and 91% for DenseNet. The accuracy for the test set was 76% for VGG16, 87% for Xception, and 91% for DenseNet. The AUC was highest for DenseNet (0.92); it was 0.83 for VGG16 and 0.91 for Xception. For the test set, the specificity and sensitivity were 0.93 and 0.84 for DenseNet, 0.89 and 0.84 for Xception, and 0.70 and 0.80 for VGG16, respectively.

Conclusion: The application of DL algorithms to intraoperative arthroscopic images has demonstrated a high level of accuracy in predicting retear occurrences.

Keywords: arthroscopic rotator cuff repair; arthroscopic imaging; deep learning; retear; prediction

Several studies have evaluated risk factors for the retear of repaired tendons after arthroscopic rotator cuff repair (ARCR), such as tear size, age, and underlying diseases, and have reported conflicting results.^{3,12,16,23,31,37} Moreover,

studies of the associations of findings on plain radiography and magnetic resonance imaging (MRI), such as critical shoulder angle and glenoid inclination angle, with the risk of retears have produced inconsistent results.^{11,13,32,45} Furthermore, several studies have evaluated rapid and accurate methods to predict retears based on patient characteristics and imaging studies; however, the results have been inconclusive.^{16,22} Fatty infiltration of the rotator cuff is one of the few consistent predictors of retears across multiple studies, as it may reflect the quality of rotator cuff tendons.^{16,18,25,26,28,42} Although no reliable objective methods are available to evaluate the tendon quality, surgeons can sometimes predict poor outcomes subjectively during tendon repair based on the tendon quality.

Artificial intelligence has improved the analysis of digital images. Several deep learning (DL)-based studies have used plain radiographs to classify proximal humeral fractures and assess subscapularis tears.^{8,17} MRI is particularly useful for developing DL algorithms that can

[†]Address correspondence to Yang-Soo Kim, MD, PhD, Department of Orthopedic Surgery, Seoul St. Mary's Hospital, The Catholic University of Korea, Banpo-Daero 222, Secho-gu, Seoul, 06591, Korea (email: kysoos@catholic.ac.kr).

*Department of Orthopedic Surgery, Seoul St. Mary's Hospital, The Catholic University of Korea, Seoul, Republic of Korea.

Submitted January 28, 2023; accepted June 12, 2023.

The authors declared that they have no conflicts of interest in the authorship and publication of this contribution. AOSM checks author disclosures against the Open Payments Database (OPD). AOSM has not conducted an independent investigation on the OPD and disclaims any liability or responsibility relating thereto.

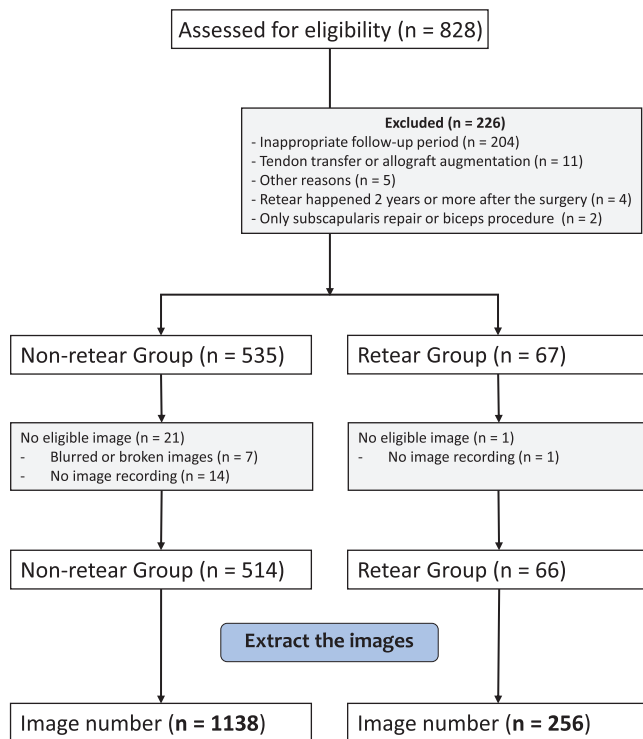


Figure 1. Flowchart of the numbers of patients and images.

identify the shoulder regions through automatic segmentation, diagnose tendon tears, and assess fatty infiltration.^{30,33,41} Computed tomography has also been used for the automatic quantification of rotator cuff muscle degeneration.³⁹ However, to the best of our knowledge, no previous study has used intraoperative ARCR images to predict the risk of retears.

The purpose of this study was to evaluate the usefulness of intraoperative arthroscopic images for the prediction of retears after ARCR using DL algorithms. We hypothesized that the tendon quality might influence the risk of retears and that DL algorithms based on arthroscopic intraoperative images can be used to assess the tendon quality and predict retears.

METHODS

Patients and Data Set

This retrospective study included patients who underwent ARCR at Seoul St. Mary's Hospital (Seoul, Korea) between January 2016 and May 2021 by a single experienced surgeon (Y.S.K.) and were followed up for >1 year with MRI. Supraspinatus tendon images at the subacromial space obtained immediately after arthroscopic repair were analyzed. Multiple images were included from the same patient when the image showed different areas of the repaired tendon.

We excluded patients who underwent tendon transfer, graft augmentation, isolated subscapularis repair or biceps procedure, or partial repair that covered <80% of the

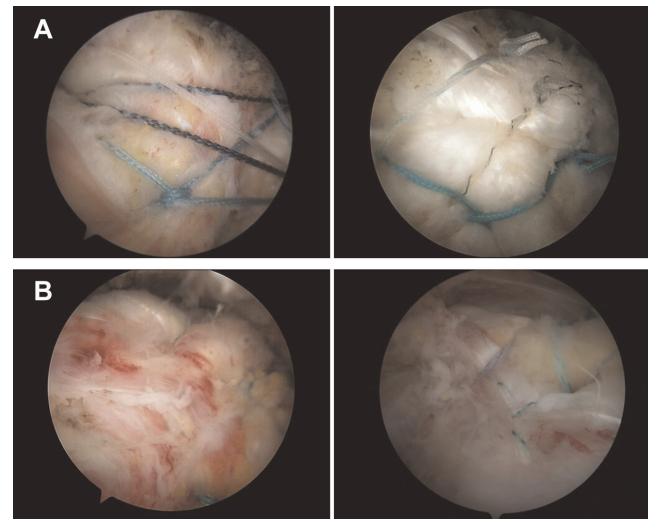


Figure 2. Representative images from the (A) nonretear and (B) retear groups.

footprint. In addition, we excluded patients for whom no arthroscopic images were available, patients with broken or blurred images, or patients with images captured from viewing portals other than the subacromial space.

Arthroscopic images were obtained from the posterolateral corner of the acromion portal using the ConMed Trinity 4K camera system. Retear was evaluated on MRI performed within 2 years after surgery because retears often occur during the early postoperative period.^{15,29} Tendon integrity on MRI was evaluated using the classification proposed by Sugaya et al,³⁷ and types IV and V were considered retears. Figure 1 shows the numbers of patients and images included in this study. Figure 2 shows representative images included in the study. This study was approved by the institutional review board of the Catholic University of Korea, Seoul St. Mary's Hospital.

Surgical Procedure and Rehabilitation

An experienced surgeon (Y.S.K.) performed the surgeries with the patients in a lateral position under general anesthesia. The repair included single-row, double-row, and suture bridge techniques. Acromioplasty, biceps procedure, and capsulectomy were performed as necessary.

Immobilization was maintained for 4 to 6 weeks postoperatively using an abduction brace. Passive range of motion (ROM) exercises were initiated after 4 to 6 weeks of immobilization. Active ROM and muscle-strengthening exercises were initiated at 8 and 12 weeks postoperatively, respectively.

Convolutional Neural Network Model Implementation

We used 3 open-source model architectures (VGG16,³⁵ DenseNet121,¹⁴ and Xception⁷) pretrained to high accuracy on the ImageNet database, which consists of 14

TABLE 1
Characteristics of Study Participants^a

| Characteristic | Nonretear Group (n = 514) | Retear Group (n = 66) | P Value |
|--|---------------------------|-----------------------|---------|
| No. of arthroscopic images | 1138 | 256 | |
| Sex, men/women, No. | 181/333 | 28/38 | .64 |
| Age, y | 61.59 ± 8.64 | 64.92 ± 6.67 | <.01 |
| Involved arm, right/left, No. | 352/162 | 49/17 | .42 |
| SSP tear size (anterior to posterior), cm | 1.18 ± 0.72 | 2.25 ± 0.93 | <.01 |
| SSP tear size (medial to lateral retraction), cm | 1.29 ± 0.85 | 2.60 ± 0.95 | <.01 |
| Full thickness/partial thickness, No. | 302/212 | 63/3 | <.01 |

^aValues are presented as mean ± SD unless otherwise indicated. SSP, supraspinatus.

million nonmedical images. We used the pretrained networks as a feature extractor and fine-tuned them using our data. We removed the last few layers from the original model and fine-tuned the parameters using additional layers. Various learning rates, images per batch, and optimizers were used to fine-tune the models.⁴⁴ The models were trained for 60 epochs using root mean square propagation as an optimizer with a learning rate of 2e−5 and binary cross-entropy loss. We resized the images to the optimal size for each model: 270 × 480 for VGG16, 224 × 224 for DenseNet121, and 229 × 229 for Xception. The accuracy graph and binary cross-entropy loss graph were used for hyperparameter optimization to avoid overfitting and underfitting.

K-fold Stratified Validation

The data set was split into training and test groups (8:2). The training group was used for K-fold stratified validation to validate the models. Because the K value was set to 3, 299 to 301 images for the nonretear group and 70 to 72 images for the retear group were used randomly for each fold. The folds were made by preserving the percentage of samples for each class so that the distribution of the data sets did not interfere.² After validating and fine-tuning the model, we evaluated the model on the test set. The test set was split before training and was not used for training or validation.

Cross-validation was described in terms of the accuracy of each fold and mean accuracy. The model performance of the test set was evaluated using the predictive accuracy, F1-score, area under the receiver operating characteristic curve (AUC), sensitivity, and specificity. The Youden J statistic was used to calculate the thresholds for specificity and sensitivity. The confusion matrices were also described. The predictive accuracy and F1 score were calculated as follows:

Predictive accuracy = $\frac{TP + TN}{TP + FP + FN + TN}$,

Positive predictive value = $\frac{TP}{TP + FP}$,

Negative predictive value = $\frac{TN}{TN + FN}$,

F1-score = $2 \times \frac{(\text{Sensitivity} \times \text{Positive predictive value})}{(\text{Sensitivity} + \text{Positive predictive value})}$,

where TP indicates a true positive, TN indicates a true negative, FP indicates a false positive, and FN indicates a false negative.

Implementation and Statistics

All models were implemented on Python (Version 3.9.12) using the Keras (Version 2.9.0) and Scikit-learn (Version 1.1.1) libraries. Our algorithms were trained and evaluated on a workstation that included NVIDIA GeForce RTX 2060 GPU and an Intel Core i7-10700 CPU. Descriptive statistics were processed using R (Version 4.0.3; R Foundation for Statistical Computing).

RESULTS

Table 1 presents the characteristics of the study participants. In total, 1394 arthroscopic intraoperative images stored on a picture archiving and communication system were obtained from 580 patients. The nonretear and retear groups included 1138 and 256 images from 514 and 66 patients, respectively (Figure 1). The mean age of the study participants was 61.59 years for the nonretear group and 64.92 years for the retear group, with a significant difference between the groups ($P < .01$). The intraoperative supraspinatus tear size in the anterior to posterior and medial to lateral directions differed significantly between the groups ($P < .01$). Full-thickness tear was the most common type in both groups, but the proportion of full-thickness tears was significantly higher in the retear group ($P < .01$). At the final follow-up (mean follow-up duration, 49 months), 27% of patients in the retear group reported a pain score of ≥5 on the visual analog scale.

Table 2 presents the 3-fold cross-validation accuracy scores by fold for each convolutional neural network (CNN) classifier model. The accuracies of the models for

TABLE 2
Accuracy of 3-Fold Cross-validation

| Algorithm | Fold 1 | Fold 2 | Fold 3 | Mean \pm SD | Test |
|-----------|--------|--------|--------|-----------------|------|
| VGG16 | 0.83 | 0.84 | 0.83 | 0.83 \pm 0.06 | 0.76 |
| DenseNet | 0.80 | 0.94 | 0.99 | 0.91 \pm 0.10 | 0.91 |
| Xception | 0.80 | 0.91 | 0.95 | 0.89 \pm 0.08 | 0.87 |

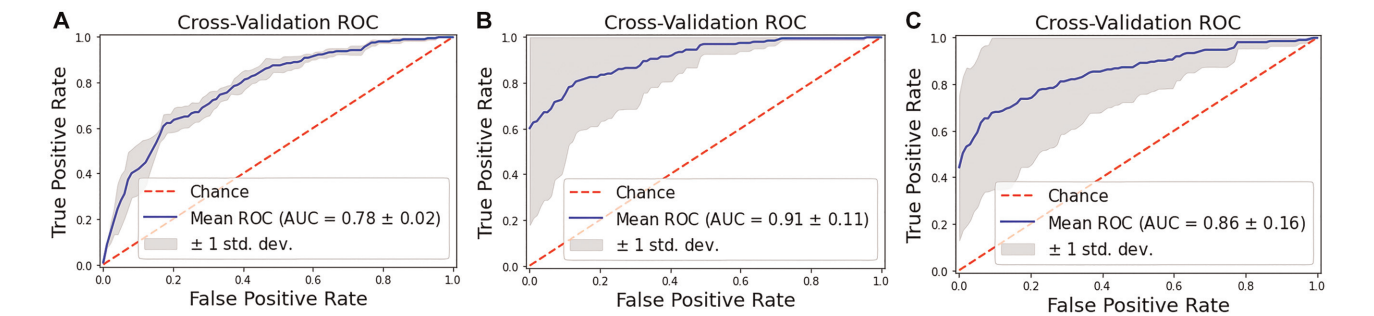


Figure 3. Results of cross-validation of the 3 models: (A) VGG16; (B) DenseNet; (C) Xception. AUC, area under the curve; ROC, receiver operating characteristic.

the test set were compared. The accuracy improved with an increase in fold number. VGG16 and Xception had mean validation accuracies of 83% and 89%, respectively. DenseNet showed the highest mean validation accuracy of 91%. The mean validation AUC values were 0.78 ± 0.02 , 0.86 ± 0.16 , and 0.91 ± 0.11 for VGG16, Xception, and DenseNet, respectively. DenseNet showed the best AUC values in the stratified validation. Figure 3 shows the receiver operating characteristic (ROC) curves during validation of the models. All 3 models showed accuracies of 80% to 90%.

The performance of each classifier model for the test set is summarized in Table 3. The test set was not included in the training validation procedure, and accuracy values for the test set were lower than the mean validation value (Table 2). The accuracies were 76%, 91%, and 87% for VGG16, DenseNet, and Xception, respectively. The AUC values for the CNN classifier using the 3 models were >0.8 . The AUC values of the VGG16 and Xception models for the test set were 0.83 and 0.91, respectively. DenseNet showed the highest AUC values for model performance (0.92). Figures 4 and 5 show the ROC curves and confusion matrices obtained for each model on the test set. The confusion matrix of DenseNet (Figure 5B) showed that the classifier correctly predicted the retear with an accuracy of $>90\%$ with intraoperative arthroscopic images.

DISCUSSION

The most important finding from the current study is that CNN classifier algorithms predicted retear based on arthroscopic images with high accuracy without the analysis of patient information or additional radiologic findings.

TABLE 3
Model Performance Using the Test Set^a

| Characteristic | VGG16 | DenseNet | Xception |
|----------------|-------|----------|----------|
| AUC | 0.83 | 0.92 | 0.91 |
| Accuracy | 0.76 | 0.91 | 0.87 |
| F1-score | 0.78 | 0.91 | 0.88 |
| Sensitivity | 0.80 | 0.84 | 0.84 |
| Specificity | 0.70 | 0.93 | 0.89 |

^aAUC, area under the curve.

The 3 CNN classifiers achieved an AUC >0.8 ; the DenseNet model predicted retear and nonretear with an accuracy of 91% and an AUC of 0.92. Our study shows the usefulness of arthroscopic images for the prediction of prognosis without the need to combine them with other factors.

Our results suggest that the postoperative prognosis can be determined based on the tendon status, thereby alleviating the need to evaluate the causes of retears. The newly developed tool allows objective communication regarding poor tendon quality and determines the risk of retears. This understanding allows the personalization of postoperative care, including the immobilization duration and rehabilitation protocol, and provides patients with appropriate caution. Furthermore, this prediction can be considered in the event of potential disputes concerning the surgeon's responsibility after the occurrence of retears. Although retears can be asymptomatic initially, they can lead to negative long-term outcomes, and the risk prediction of retear could be used to tailor the follow-up duration. Notably, a high probability of retear, as indicated by the algorithm, does not imply surgical failure or render the

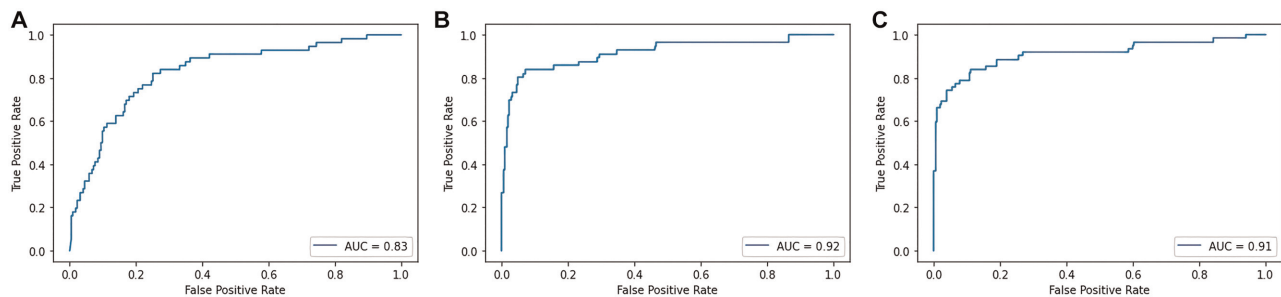


Figure 4. Receiver operating characteristic curves for the test set for the 3 models: (A) VGG16; (B) DenseNet; (C) Xception. AUC, area under the curve.

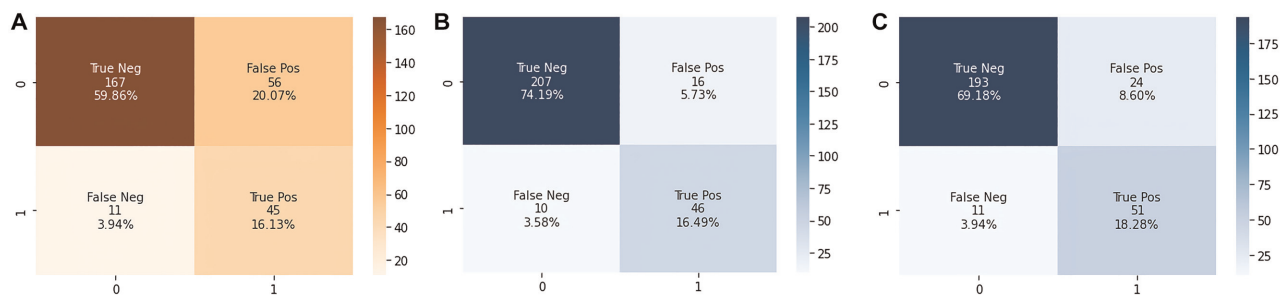


Figure 5. Confusion matrices for the 3 models: (A) VGG16 ; (B) DenseNet; (C) Xception. AUC, area under the curve; Neg, negative; Pos, positive.

surgery unnecessary because retear is not the only important surgical outcome.

In our study, intraoperative arthroscopic images predicted retears without using demographic or additional factors such as age, comorbidities, and tear size. Although multiple studies have explored predictors of retears after ARCR based on patient characteristics, such as age, sex, smoking status, and underlying disease, the results have been contradictory, and only a few factors have been established as prognostic indicators.^{1,5,6,9,10,16,20,22,23} Multiple parameters from plain radiographs, such as critical shoulder angle, acromion index, and lateral acromial angle, showed no relationships with retears.^{11,13,43} Studies of the usefulness of MRI-related factors, such as tear size, fatty infiltration, and muscle atrophy as prognostic indicators, have demonstrated relatively few discrepancies.^{4,16,18,20,21,24,34} Compared with patient and plain radiograph factors, MRI-related factors are direct and more accurate indicators of tendon status. Tendon quality is an important predictor of retears, and repair failure often involves sutures cutting through the tendon, regardless of suture technique.²⁷ Therefore, intraoperative arthroscopic images could be accurate predictors of retears because they provide direct visualization of the tendon quality compared with other existing factors. Moreover, no reliable quantitative methods exist to assess tendon quality. However, with the increasing use of DL algorithms, images can be transformed into numerical data for analysis.

Similar to arthroscopic images in orthopaedic surgery, the analysis of endoscopic images using DL also shows

promising results. Song et al³⁶ proposed a DL model to classify the mucosal surface patterns of colon polyps with high accuracy, which was confirmed by histopathology analysis. In addition to prediction and classification, DL-based detection or segmentation using endoscopic images has also been studied. For instance, Urban et al⁴⁰ showed the usefulness of a DL algorithm to detect nonpolypoid polyps, which is challenging even for experts. However, computed tomography and MRI are the main tools to evaluate and predict the prognosis after shoulder surgery. Because ARCR is one of the most commonly performed in orthopaedic surgeries, arthroscopic images may be useful for the prediction of prognosis, similar to endoscopic images.


One of the goals of artificial intelligence is to assist humans in image interpretation. Several studies have found that DL is superior to experts in terms of the interpretation of images.^{4,38} For example, Sultan et al³⁸ developed a DL system that identifies shoulder arthroplasty implants on plain radiographs and compared it with a human expert. This algorithm was shown to be useful to less experienced and even experienced surgeons for the identification of previously inserted implants before revision surgery. Although humans were able to identify implants in this case, the DL system may be useful for cases in which humans are unable to identify any radiologic relationship or pattern. Computer vision on occasion outperforms humans in identifying more complex and subtle patterns.^{4,19} Therefore, DL-based algorithms are expected to become more useful for interpreting a variety of images.

Our study had certain limitations. First, the images used in our study focused on rotator cuff status at the time of the operation. Because we used intraoperative images, the patients had already undergone surgery at the time of application of this model. Therefore, this model cannot predict retear occurrence preoperatively. In addition, postoperative factors could not be evaluated on the arthroscopic images. Second, surgeons debride the tendon using various means, including electrocautery. Therefore, arthroscopic images obtained before and after debridement may have certain differences. However, debridement does not affect tendon quality, so a poor-quality tendon with debridement is not similar to a healthy-quality tendon. Therefore, debridement may have a negligible effect on outcome, considering the high-accuracy results of the test set. Third, the study had a retrospective design. In addition, a large number of retear images can increase the accuracy. Finally, no external validation set was used for this study. However, the test set was not involved in training and validation.

CONCLUSION

DL algorithms based on intraoperative arthroscopic images can predict retears after ARCR with high accuracy and without the analysis of other factors. The ability to predict retears may depend on the tendon quality visible on intraoperative arthroscopic images.

ORCID iDs

Sung-Hyun Cho  <https://orcid.org/0000-0002-2834-0627>
Yang-Soo Kim  <https://orcid.org/0000-0003-4267-7880>

REFERENCES

1. Beason DP, Tucker JJ, Lee CS, Edelstein L, Abboud JA, Soslowsky LJ. Rat rotator cuff tendon-to-bone healing properties are adversely affected by hypercholesterolemia. *J Shoulder Elbow Surg.* 2014;23(6):867-872.
2. Bey R, Goussault R, Grolleau F, Benchoufi M, Porcher R. Fold-stratified cross-validation for unbiased and privacy-preserving federated learning. *J Am Med Inform Assoc.* 2020;27(8):1244-1251.
3. Bishop J, Klepps S, Lo IK, Bird J, Gladstone JN, Flatow EL. Cuff integrity after arthroscopic versus open rotator cuff repair: a prospective study. *J Shoulder Elbow Surg.* 2006;15(3):290-299.
4. Buetti-Dinh A, Galli V, Bellenberg S, et al. Deep neural networks outperform human expert's capacity in characterizing bioleaching bacterial biofilm composition. *Biotechnol Rep (Amst).* 2019;22:e00321.
5. Charousset C, Bellaiche L, Kalra K, Petrover D. Arthroscopic repair of full-thickness rotator cuff tears: is there tendon healing in patients aged 65 years or older? *Arthroscopy.* 2010;26(3):302-309.
6. Cho NS, Rhee YG. The factors affecting the clinical outcome and integrity of arthroscopically repaired rotator cuff tears of the shoulder. *Clin Orthop Surg.* 2009;1(2):96-104.
7. Chollet F. Xception: deep learning with depthwise separable convolutions. In: *Proceedings of the IEEE Conference on Computer Vision and Pattern Recognition.* CVPR Open Access. 2017:1251-1258. https://openaccess.thecvf.com/content_cvpr_2017/html/Chollet_Xception_Deep_Learning_CVPR_2017_paper.html
8. Chung SW, Han SS, Lee JW, et al. Automated detection and classification of the proximal humerus fracture by using deep learning algorithm. *Acta Orthop.* 2018;89(4):468-473.
9. Chung SW, Kim JY, Kim MH, Kim SH, Oh JH. Arthroscopic repair of massive rotator cuff tears: outcome and analysis of factors associated with healing failure or poor postoperative function. *Am J Sports Med.* 2013;41(7):1674-1683.
10. Chung SW, Oh JH, Gong HS, Kim JY, Kim SH. Factors affecting rotator cuff healing after arthroscopic repair: osteoporosis as one of the independent risk factors. *Am J Sports Med.* 2011;39(10):2099-2107.
11. Como CJ, Hughes JD, Lesniak BP, Lin A. Critical shoulder angle does not influence retear rate after arthroscopic rotator cuff repair. *Knee Surg Sports Traumatol Arthrosc.* 2021;29(12):3951-3955.
12. Galatz LM, Ball CM, Teefey SA, Middleton WD, Yamaguchi K. The outcome and repair integrity of completely arthroscopically repaired large and massive rotator cuff tears. *J Bone Joint Surg Am.* 2004;86(2):219-224.
13. Garcia GH, Liu JN, Degen RM, et al. Higher critical shoulder angle increases the risk of retear after rotator cuff repair. *J Shoulder Elbow Surg.* 2017;26(2):241-245.
14. Huang G, Liu Z, Van Der Maaten L, Weinberger KQ. Densely connected convolutional networks. In: *Proceedings of the IEEE Conference on Computer Vision and Pattern Recognition.* CVPR Open Access. 2017:4700-4708. https://openaccess.thecvf.com/content_cvpr_2017/html/Huang_Densely_Connected_Convolutional_CVPR_2017_paper.html
15. Iannotti JP, Deutsch A, Green A, et al. Time to failure after rotator cuff repair: a prospective imaging study. *J Bone Joint Surg Am.* 2013;95(11):965-971.
16. Jeong HY, Kim HJ, Jeon YS, Rhee YG. Factors predictive of healing in large rotator cuff tears: is it possible to predict retear preoperatively? *Am J Sports Med.* 2018;46(7):1693-1700.
17. Kang Y, Choi D, Lee KJ, Oh JH, Kim BR, Ahn JM. Evaluating subscapularis tendon tears on axillary lateral radiographs using deep learning. *Eur Radiol.* 2021;31(12):9408-9417.
18. Khair MM, Lehman J, Tsouris N, Gulotta LV. A systematic review of preoperative fatty infiltration and rotator cuff outcomes. *HSS J.* 2016;12(2):170-176.
19. Khosla A, An B, Lim JJ, Torralba A. Looking beyond the visible scene. In: *Proceedings of the IEEE Conference on Computer Vision and Pattern Recognition.* CVPR Open Access. 2014:3710-3717. https://www.cv-foundation.org/openaccess/content_cvpr_2014/html/Khosla_Looking_Beyond_the_2014_CVPR_paper.html
20. Kim DM, Jeon IH, Yang HS, et al. Poor prognostic factors in patients with rotator cuff retear. *Orthop J Sports Med.* 2021;9(4):2325967121992154.
21. Kim JY, Zhong Z, Lee HW, Lee GW, Noh KC. Quantitative magnetic resonance imaging measurement of muscle atrophy and fatty degeneration after arthroscopic rotator cuff repair. *J Orthop Surg (Hong Kong).* 2022;30(2):10225536221095276.
22. Kwon J, Kim SH, Lee YH, Kim TI, Oh JH. The rotator cuff healing index: a new scoring system to predict rotator cuff healing after surgical repair. *Am J Sports Med.* 2019;47(1):173-180.
23. Le BT, Wu XL, Lam PH, Murrell GA. Factors predicting rotator cuff retears: an analysis of 1000 consecutive rotator cuff repairs. *Am J Sports Med.* 2014;42(5):1134-1142.
24. Lee S, Lucas RM, Lansdown DA, et al. Magnetic resonance rotator cuff fat fraction and its relationship with tendon tear severity and sub-ject characteristics. *J Shoulder Elbow Surg.* 2015;24(9):1442-1451.
25. Lee YS, Jeong JY, Park CD, Kang SG, Yoo JC. Evaluation of the risk factors for a rotator cuff retear after repair surgery. *Am J Sports Med.* 2017;45(8):1755-1761.
26. Lobo-Escobar L, Ramazzini-Castro R, Codina-Grano D, Lobo E, Minguel-Monyart J, Ardevol J. Risk factors for symptomatic retears after arthroscopic repair of full-thickness rotator cuff tears. *J Shoulder Elbow Surg.* 2021;30(1):27-33.
27. Mazzocca AD, Millett PJ, Guanche CA, Santangelo SA, Arciero RA. Arthroscopic single-row versus double-row suture anchor rotator cuff repair. *Am J Sports Med.* 2005;33(12):1861-1868.

28. McElvany MD, McGoldrick E, Gee AO, Neradilek MB, Matsen FA III. Rotator cuff repair: published evidence on factors associated with repair integrity and clinical outcome. *Am J Sports Med.* 2015;43(2):491-500.
29. Miller BS, Downie BK, Kohen RB, et al. When do rotator cuff repairs fail? Serial ultrasound examination after arthroscopic repair of large and massive rotator cuff tears. *Am J Sports Med.* 2011;39(10):2064-2070.
30. Ro K, Kim JY, Park H, et al. Deep-learning framework and computer assisted fatty infiltration analysis for the supraspinatus muscle in MRI. *Sci Rep.* 2021;11(1):15065.
31. Saccomanno MF, Sircana G, Cazzato G, Donati F, Randelli P, Milano G. Prognostic factors influencing the outcome of rotator cuff repair: a systematic review. *Knee Surg Sports Traumatol Arthrosc.* 2016;24(12):3809-3819.
32. Scheiderer B, Imhoff FB, Johnson JD, et al. Higher critical shoulder angle and acromion index are associated with increased retear risk after isolated supraspinatus tendon repair at short-term follow up. *Arthroscopy.* 2018;34(10):2748-2754.
33. Shim E, Kim JY, Yoon JP, et al. Automated rotator cuff tear classification using 3D convolutional neural network. *Sci Rep.* 2020;10(1):15632.
34. Shin YK, Ryu KN, Park JS, Jin W, Park SY, Yoon YC. Predictive factors of retear in patients with repaired rotator cuff tear on shoulder MRI. *AJR Am J Roentgenol.* 2018;210(1):134-141.
35. Simonyan K, Zisserman A. Very deep convolutional networks for large-scale image recognition. arXiv preprint arXiv:14091556. 2014. <https://arxiv.org/abs/1409.1556>
36. Song EM, Park B, Ha CA, et al. Endoscopic diagnosis and treatment planning for colorectal polyps using a deep-learning model. *Sci Rep.* 2020;10(1):30.
37. Sugaya H, Maeda K, Matsuki K, Moriishi J. Repair integrity and functional outcome after arthroscopic double-row rotator cuff repair: a prospective outcome study. *J Bone Joint Surg Am.* 2007;89(5):953-960.
38. Sultan H, Owais M, Park C, Mahmood T, Haider A, Park KR. Artificial intelligence-based recognition of different types of shoulder implants in X-ray scans based on dense residual ensemble-network for personalized medicine. *J Personalized Med.* 2021;11(6):482.
39. Taghizadeh E, Truffer O, Becce F, et al. Deep learning for the rapid automatic quantification and characterization of rotator cuff muscle degeneration from shoulder CT datasets. *Eur Radiol.* 2021;31(1):181-190.
40. Urban G, Tripathi P, Alkayali T, et al. Deep learning localizes and identifies polyps in real time with 96% accuracy in screening colonoscopy. *Gastroenterology.* 2018;155(4):1069-1078.e1068.
41. Wang G, Han Y. Convolutional neural network for automatically segmenting magnetic resonance images of the shoulder joint. *Comput Methods Programs Biomed.* 2021;200:105862.
42. Wu XL, Briggs L, Murrell GA. Intraoperative determinants of rotator cuff repair integrity: an analysis of 500 consecutive repairs. *Am J Sports Med.* 2012;40(12):2771-2776.
43. Xie L, Xu X, Ma B, Liu H. A high acromion-greater tuberosity impingement index increases the risk of retear after arthroscopic rotator cuff repair. *J Orthop Surg (Hong Kong).* 2022;30(1):10225536221092219.
44. Yang L, Shami A. On hyperparameter optimization of machine learning algorithms: theory and practice. *Neurocomputing.* 2020;415:295-316.
45. Zhao J, Luo M, Pan J, et al. Risk factors affecting rotator cuff retear after arthroscopic repair: a meta-analysis and systematic review. *J Shoulder Elbow Surg.* 2021;30(11):2660-2670.